Applied Geochemistry 61 (2015) 109–118

Contents lists available at ScienceDirect

Applied Geochemistry

journal homepage: www.elsevier.com/locate/apgeochem

The dissolution of olivine added to soil: Implications for enhanced weathering

P. Renforth [a,b,*], P.A.E. Pogge von Strandmann [b,c], G.M. Henderson [b]

[a] School of Earth and Ocean Sciences, Cardiff University, Cardiff CF10 3AT, UK
[b] Department of Earth Sciences, University of Oxford, South Parks Road, Oxford OX1 3AN, UK
[c] Institute of Earth and Planetary Sciences, University College London and Birkbeck, University of London, Gower Street, London WC1E 6BT, UK

ARTICLE INFO

Article history:
Available online 27 May 2015
Editorial handling by M. Kersten

ABSTRACT

Chemical weathering of silicate minerals consumes atmospheric CO_2 and is a fundamental component of geochemical cycles and of the climate system on long timescales. Artificial acceleration of such weathering ("enhanced weathering") has recently been proposed as a method of mitigating anthropogenic climate change, by adding fine-grained silicate materials to continental surfaces. The efficacy of such intervention in the carbon cycle strongly depends on the mineral dissolution rates that occur, but these rates remain uncertain. Dissolution rates determined from catchment scale investigations are generally several orders of magnitude slower than those predicted from kinetic information derived from laboratory studies. Here we present results from laboratory flow-through dissolution experiments which seek to bridge this observational discrepancy by using columns of soil returned to the laboratory from a field site. We constrain the dissolution rate of olivine added to the top of one of these columns, while maintaining much of the complexity inherent in the soil environment. Continual addition of water to the top of the soil columns, and analysis of elemental composition of waters exiting at the base was conducted for a period of five months, and the solid and leachable composition of the soils was also assessed before and after the experiments. Chemical results indicate clear release of Mg^{2+} from the dissolution of olivine and, by comparison with a control case, allow the rate of olivine dissolution to be estimated between $10^{-16.4}$ and $10^{-15.5}$ moles(Mg) cm^{-2} s^{-1}. Measurements also allow secondary mineral formation in the soil to be assessed, and suggest that no significant secondary uptake of Mg^{2+} has occurred. The olivine dissolution rates are intermediate between those of pure laboratory and field studies and provide a useful constraint on weathering processes in natural environments, such as during soil profile deepening or the addition of mineral dust or volcanic ash to soils surfaces. The dissolution rates also provide critical information for the assessment of enhanced weathering including the expected surface-area and energy requirements.

1. Introduction

Weathering of silicate rocks at the Earth's surface consumes CO_2 and releases nutrients to fuel the biological cycle. As such, weathering is one of the fundamental geochemical processes shaping the evolution and environment of the planet. On long timescales, silicate weathering provides the ultimate sink for CO_2 released by volcanic degassing and, because the rate of such weathering is temperature dependent, this sink is thought to respond to climate change to provide a strong negative feedback stabilising the Earth's climate (e.g. Berner and Kothavala, 2001; Walker et al., 1981). As such, silicate weathering is likely to have been the fundamental process that maintained the Earth's climate within the narrow bands necessary for life for several billion years. An increase in global weathering rates is expected in response to anthropogenic warming and this increased weathering will ultimately (on the timescale of hundreds of thousands of years) serve to remove CO_2.

Despite considerable work in recent decades, significant gaps in understanding natural weathering remain. Unpacking the mechanisms that control weathering at a catchment and global scale has proved difficult. Laboratory investigations have shown that dissolution rates (W_r) are a function of temperature (T; e.g. White et al., 1999), mineral saturation (Ω; e.g. Nagy et al., 1991), pH (e.g. Pokrovsky and Schott, 2000) and mineral surface area (SA e.g. Holdren and Speyer, 1985), and these relationships can be collected into a single, well tested, expression (e.g. Eq. (1)).

$$W_r = SA \cdot k \cdot e^{\frac{E}{RT}} a_{H^+} (1 - \Omega) \quad (1)$$

* Corresponding author. Tel.: +44 (0) 29 208 79672; fax: +44 (0) 29 208 74326.
E-mail address: RenforthP@Cardiff.ac.uk (P. Renforth).

http://dx.doi.org/10.1016/j.apgeochem.2015.05.016
0883-2927/

where k is a dissolution rate constant (Palandri and Kharaka, 2004). However, applying this relationship to investigate weathering on a field scale has persistently produced dissolution rates that are several orders of magnitude slower than determined in laboratory experiments (see White and Brantley, 1995 and references therein). It is difficult to isolate the variables in Eq. (1) in the field, and what is measured (through analysis of drainage or soil pore waters) is their combined and attenuated effect. Assumptions regarding the density of the mineral and the depth of the weathering zone (e.g. Calmels et al., 2011) are necessary to convert a spatially explicit rate (e.g. in moles km^{-2} $year^{-1}$) into one that is normalised to mineral surface area (e.g. in moles cm^{-2} s^{-1}). These assumptions can result in large uncertainties in rates. Furthermore, the proportion of the surface area that is actively weathering may change over time as a result of encapsulation in secondary mineral precipitation or formation of a cation depleted/silica rich surface layer (White and Brantley, 2003). The hydraulics and biogeochemistry of soils are complex. Intermittent rainfall, and/or evapotranspiration, may result in soil pore water becoming saturated or oversaturated with minerals. Soil pH may fluctuate as a function of rapidly evolving carbon dioxide partial pressure (see Manning and Renforth (2012) for summary) or organic compound degradation and exudation (particularly low molecular mass organic acids; van Hees et al., 2000). Imprinted over these natural processes may be additional weathering from human activity (e.g. tilling and irrigation, Pačes, 1983). A major challenge for weathering research is the ability to derive meaning in the outputs of short-term highly controlled laboratory studies for complex natural environments.

The lack of understanding of the controls on weathering in the field, and the limited available dissolution kinetic data on minerals intentionally added to the environment, means that it is not possible to predict with any accuracy the rate of chemical weathering (or the fate of resulting solutes) that would result from any intentional manipulation of soil weathering. Such manipulation, sometimes termed, 'enhanced weathering' (Hartmann et al., 2013), has been considered as a method of removing CO_2 from the atmosphere by applying crushed minerals to the land surface (Schuiling and Krijgsman, 2006; Manning, 2008; Renforth, 2012; Köhler et al., 2010; Moosdorf et al., 2014), to the ocean (Harvey, 2008; Köhler et al., 2013; Kheshgi, 1995; Renforth et al., 2013), or to coastal zones (Hangx and Spiers, 2009; Schuiling and de Boer, 2010). It is anticipated that the weathering products and sequestered carbon from all of these proposals will be transported to the ocean, which already have a considerable residence time (e.g. 10^5 years, see Rau, 2011). The uncertainty in dissolution kinetics is one of the primary reasons why, in recent literature, it has been possible for various workers to suggest that accelerated weathering might be used to remove several billion tonnes (Pg) of CO_2 from the atmosphere per year (Schuiling and Krijgsman, 2006), while others have suggested that enhanced weathering is limited by mineral saturation and may have restricted use for intentional CO_2 removal (Hartmann et al., 2013; Köhler et al., 2010). The goal of this study was to test an experimental method that may be used to obtain robust dissolution rate data for minerals intentionally added to soils.

Only a limited number of studies have investigated the dissolution rate of minerals intentionally added to the environment. Peters et al. (2004) investigated changes in stream chemistry due to the addition of 50 tonnes of ground wollastonite ($CaSiO_3$) onto the Hubbard Brooke catchment, US. The authors noted an increase in the concentration of Ca in the stream draining the catchment, and attributed this to the dissolution of the added mineral. Surface-area-normalised dissolution rates were between 10^{-15} and 10^{-20} moles cm^{-2} s^{-1}. Because the majority of the solution in the Hubbard Brooke watercourse is derived from shallow groundwater, (and lysimeters placed in the soil showed little contribution of the distributed wollastonite to the groundwater), it is thought that the chemical response to the addition is a result of dissolution of the material that fell initially into the watercourse (about 1.5% of the total). Manning et al. (2013) were able to calculate a single minimum dissolution rate of 10^{-16} moles cm^{-2} s^{-1} for crushed dolerite that was weathered in an artificial soil created using quarry fines mixed with organic materials (food industry waste and compost). They inferred a mass balance of calcium from mineral carbonate formation; the actual dissolution rate is therefore poorly constrained. In a growth experiment (closed soil system) ten Berge et al. (2012) measured the change in water soluble Mg to determine a dissolution rate of olivine between 10^{-14} and 10^{-16} moles cm^{-2} s^{-1}. While this approach provided a dissolution rate, it did not fully quantify the magnesium efflux from the soil, and potentially over estimates the contribution to carbon sequestration. There is a need to develop an experimental approach capable of constraining a budget for weathering products while maintaining the complexity of soils.

2. Overview of experimental design

In this study, the complexity of the natural environment was brought into the controlled laboratory by extracting soil cores from arable agricultural land and establishing them as lysimeters in the laboratory (Lundström, 1990, Sigfusson et al., 2006). Crushed and ground olivine was added to the top of one soil core, and a nutrient solution was drip-fed into the top and collected at the base. This approach allows complex soil processes to be replicated in the laboratory, while providing enough control to develop a closed budget for olivine dissolution without fully deconstructing the effect of complex soil biogeochemistry. By comparing the effluent solutions from the olivine-modified core with those from a control core, we account for the background signal and assess the dissolution rate of the added olivine.

3. Experimental methods

3.1. Site description and soil core extraction

In May 2012, 3 soil cores (contained in an acrylic plastic tube 0.1×1.0 m) were extracted from an agricultural field in North Oxfordshire using a premier Compact 110 percussion window sampler (Perdiswell Farm; 1°19′50.03″W, 51°51′27.55″N, Fig. 1A). The location at the time was used for growing *Vicia faba* (broad bean), and had previously been used for a range of arable crops (e.g. *Triticium* sp., wheat). The soil overlies Jurassic limestone and mudstone from the Great Oolite Group, and has been in agricultural use for over 100 years. The soils were calcareous with a thin (10–15 cm) organic rich plough layer, underlain by weakly differentiated subsoil and parent material (Fig. 1B and C) to 1 m depth.

3.2. Soil chemical analysis

Soil was removed at 5 cm depth intervals from one of the cores, oven dried for 24 h (the moisture content assessed by mass loss during drying), and the fine fraction (<2 mm) was separated. XRF analysis was conducted using a PANalytical Axios Advanced XRF spectrometer for major elements (University of Leicester) calibrated using BCS375, BCS376, and BCS372/1 standards. To analyse the elemental composition of the exchanged cations, carbonate phases and bulk soil respectively, steps 1 (1 M Sodium Acetate), 2 (1 M Acetic Acid) and 5 (concentrated HF) of a sequential leach were performed using the method outlined in Tessier et al. (1979). For organic (TOC) and inorganic (TIC) carbon determination, 2 aliquots of each sample (one of which was ashed at 450 °C overnight to remove organic carbon) were introduced into

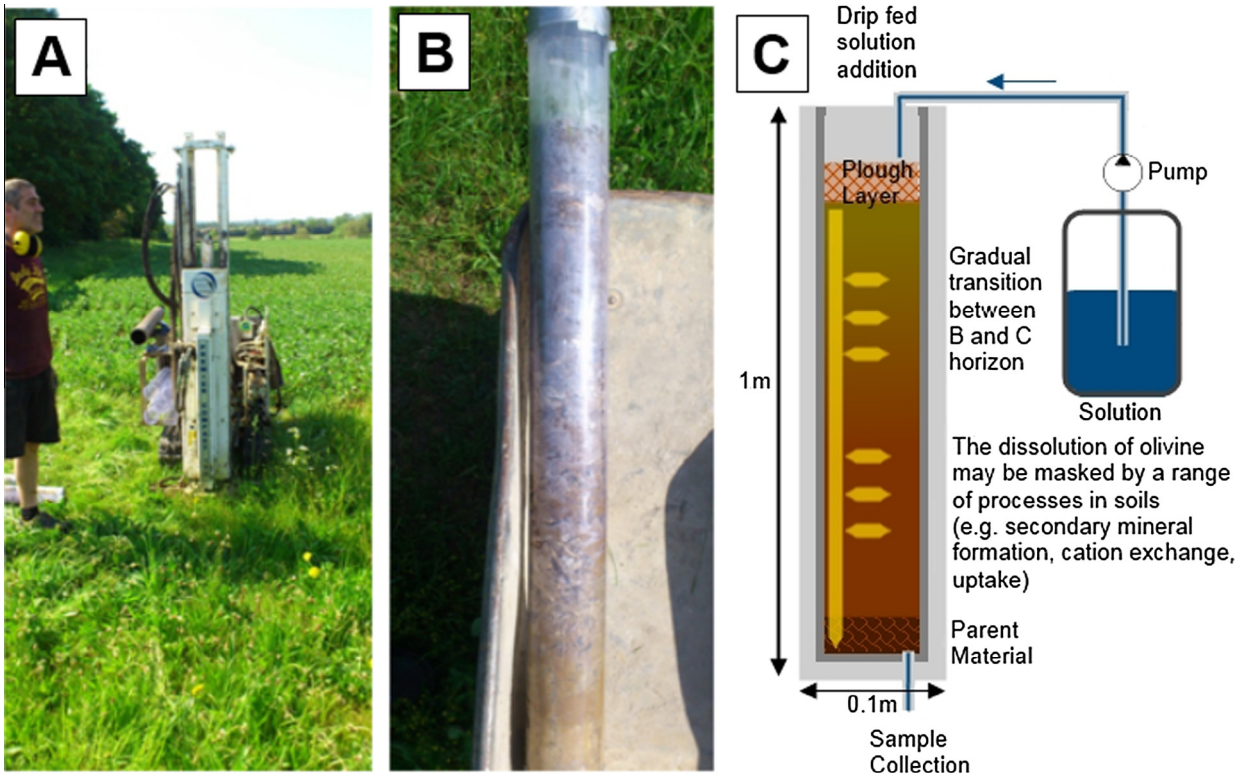

Fig. 1. Photograph showing the extraction (A) and (1 m) profile (B) of the soil core and a conceptual diagram of the experimental setup (C).

a tube furnace at 1200 °C flushed with pure-O_2 gas. A fraction of the resulting gas stream was transferred to Coulomat 750 (Ströhlein Instruments, Oxford), and analysed through titration in an $Ba(OH)_2$ electrolysis cell. The unit has an analytical precision of ±0.9% and ±2.1% for organic and inorganic carbon respectively. The remaining soil cores were stored for 6 months at 5 °C.

3.3. Olivine characterisation

Olivine was obtained from the Åheim plant in Møre og Romsdal county (Western Norway, from Minelco Ltd.). The material was ground using a tungsten carbide tema mill (University of Birmingham), and the particle size distribution was analysed by dry sieving (Table 1). 78% of the olivine had a particle diameter greater than 125 μm. Although scanning electron microscopy (JEOL JSM-840A Scanning electron microscope fitted with a secondary electron detector; Oxford) images revealed the presence of ultrafine <5 μm particles adhered to the surface of the olivine (Fig. 2A and B). Surface area of the olivine was determined by N_2 absorption using a Micromeretics Gemini VI (Oxford) and XRF analysis was conducted as described above (Table 1). The olivine had a forsterite (Mg_2SiO_4) composition of greater than 80%, when assuming the Mg content (from XRF analysis) is wholly derived from this phase.

Table 1
Characterisation of olivine.

BET surface area ($m^2\ g^{-1}$)	3.04 ± 0.03
Particle size distribution	Mass%
>500 μm	7.4
500–212 μm	27.5
212–125 μm	50.0
125–63 μm	11.1
63–45 μm	3.1
<45 μm	0.8
Total	99.9
XRF analysis	Mass%
SiO_2	41.64
TiO_2	0.02
Al_2O_3	0.75
Fe_2O_3 (total)	7.39
MnO	0.11
MgO	47.73
CaO	0.38
Na_2O	<0.01
K_2O	0.05
P_2O_5	0.01
SO_3	<0.01
Loss on ignition	2.27
Total	100.29

3.4. Laboratory setup

Two of these soil cores were mounted vertically in a 19 °C temperature-controlled laboratory (e.g. Fig. 1C; herein referred to as 'columns'). The top 0.2 m of each column was removed, mixed by hand, and returned to the column. Prior to reintroduction, 100 g of crushed and ground olivine was added to one of the mixes. Herein this will be referred to as 'olivine treatment'; in the 'control' the soil was replaced without olivine addition. Over 5 months, a modified Hoagland nutrient solution (~200 ppm K, N, 30 ppm P, 37 ppb Ca, 30 ppb S), was drip fed into the top of the columns using a 2 channel peristaltic pump at 15 ml h^{-1}, and samples were collected every 1–2 days at the base, filtered (Whatmann 0.2 μm cellulose nitrate filter), and acidified for ICP-MS analysis. The experiment was temporally suspended for 20 days between December 2012 and January 2013. It took approximately 3 days for the column to fill and empty, which suggests a total pore water volume of ~1 l (equivalent to a typical soil porosity of 15%).

After 5 months the experiment was terminated by switching off the peristaltic pump and the columns were left to drain over

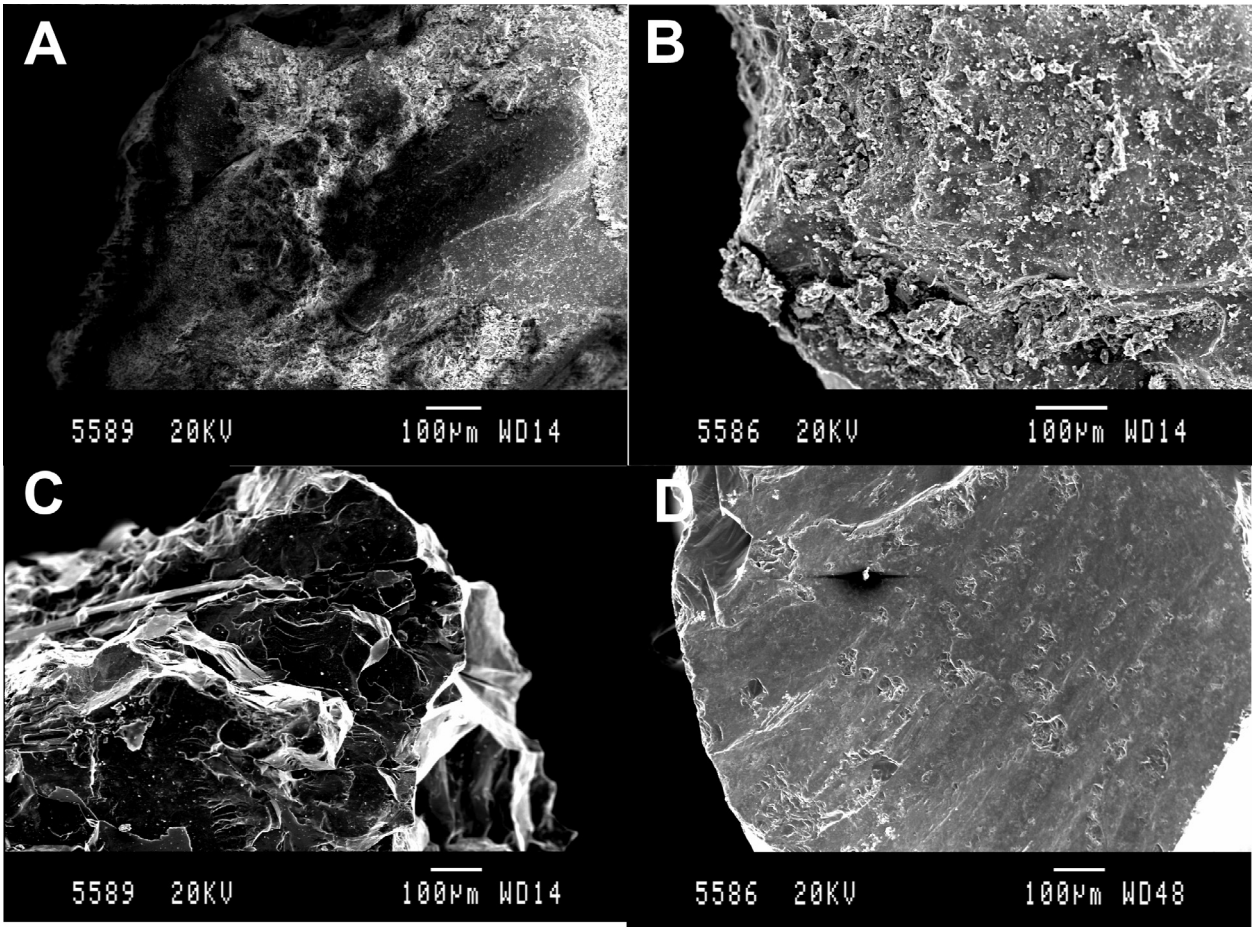

Fig. 2. Scanning electron microscope images of crushed 'raw' olivine used in the experiment unsonicated (A) and following sonication (B), and olivine picked from the top of the soil column following the experiment (C) and following sonication (D).

2 days. Soil from these columns was removed at 5 cm depth intervals, oven dried for 24 h, the fine fraction separated, and analysed according to the protocols set out above for the 'initial material'.

3.5. Solution analysis

Solutions exiting the soil columns were collected every 1–2 days and concentrations of Si, Mg, Ca, Al, Cr, and Fe were determined using a sector-field inductively coupled plasma mass spectrometer (Thermo Element 2; Oxford) calibrated using internal calibration solutions mixed from high-purity single element solutions. Accuracy was assessed by analysing the international reference standards SLRS-5 and IAPSO for pore waters, and BHVO-2 and SGR-1b for solids. Levels of Quantitation (in $ng\,g^{-1}$) for each element 0.360 (Mg), 0.168 (Al), 90.7 (Ca), 5.63 (Si), 0.096 (Cr), and 0.104 (Fe) for the first 45 days. Between 45 and 133 days, the levels of quantitation were 0.344 (Mg), 0.202 (Al), 158 (Ca), 4.71 (Si), 0.144 (Cr), and 0.070 (Fe). Analytical precision (in %) was 4.52 (Mg), 2.66 (Al), 3.52(Ca), 19.3 (Si), 2.94 (Cr), and 1.01 (Fe).

4. Results

4.1. Solution time series

Over 133 days, 49 l of solution was passed through the columns. Fig. 3 presents the concentration of major and trace cations in the effluent solutions. Mg and Ca concentrations decreased in the solution from both columns (from $\sim 7 \pm 0.3$ mgMg l^{-1} and $\sim 450 \pm 15$ mgCa l^{-1}), whereas Al and Si remained largely unchanged (0.2 ± 0.1 mg l^{-1}, and 1.9 ± 0.5 mg l^{-1} respectively), with no significant difference between treatment and control. The Mg content of solutions from the olivine treated column was consistently greater than that in the control, and elevated to approximately 4.5 ± 0.1 mg l^{-1} by the end of the experiment. The pH of the input solution varied widely (between 6.5 and 8.3), but had little effect on the pH of the effluent solutions (7.2 for the olivine treatment; 7.5 for the control; ±0.2).

This concentration and solution flux constitutes an approximate mass loss of 15.1 g Ca (11.6 g for the control), 0.3 g Mg (0.2 for the control), 0.1 g Si, 10 mg Al, 0.7 mg Fe, and 83 µg Cr (60 µg for the control).

4.2. Soil total elemental and exchangeable cation composition

The major elemental composition of the soil columns is presented in Table S1 in the Supporting Information (loss on ignition generally agreed with the TOC + TIC). As expected, elevated magnesium concentrations (~3.7% MgO) were detected in the top 10 cm of the olivine treated soil following the experiment. Below this, the soil was similar to the control and initial material, suggesting minimal transport of the crushed silicate through the soil column. The potassium concentration was elevated in the olivine treated (16.7% K_2O) and control (16.0% K_2O) columns relative to the initial material (12.0% K_2O) suggesting that the potassium in the input solution had adsorbed onto exchange sites in the soil or precipitated in secondary minerals.

The total calcium concentration scales linearly with TIC (Fig. 4A) suggesting that it is largely derived from a carbonate phase. The

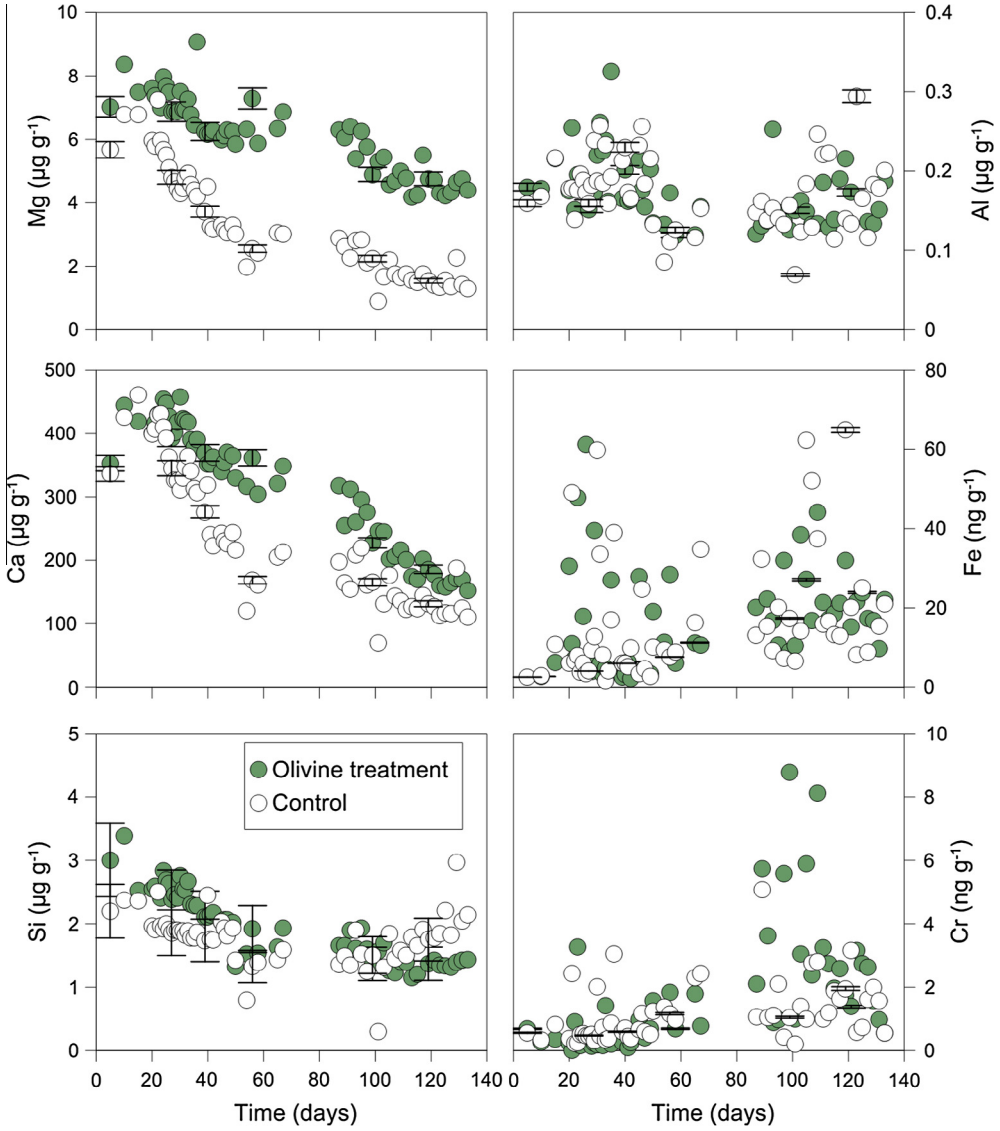

Fig. 3. Column effluent solution analysis time series. All Mg, Ca, Si, Al and Fe values are significantly above the limit of quantitation. The LoQ for Cr is 0.144 ng g^{-1}.

total magnesium concentration appears to have no relationship with TIC (Fig. 4B), which suggests the carbonate phase is composed primarily of $CaCO_3$ with only a small amount of $MgCO_3$ (~1.5 ngMg g^{-1}; confirmed in step 2 of the sequential extraction), and the majority of magnesium is likely to be contained as a minor constituent within a Si–Al phase.

Concentration profiles of exchangeable cations in the initial soil material (measured through sodium acetate leaching) are presented in Table S3 in the Supporting Information. Magnesium is the largest component and decreases with depth from 100 µg g^{-1} near the surface to <10 µg g^{-1} at the base. Fe and Ca decrease with depth from 5 µg g^{-1} at the surface to 2 µg g^{-1} at the base. Cr and Ni remain relatively constant with depth at 1.6 and 0.1 µg g^{-1} respectively. Following the experiment the exchangeable Mg decreased by 73% and 8% in the control and olivine treatment respectively (although the reduction in the olivine treated column is not statistically significant, Table S4).

4.3. Soil profiles

Between 0 and 30 cm depth, the TIC was between 0% and 3% in all three columns. Below this, the concentrations were considerably more variable (0.2–7.1%). Compared to the initial soil, the control and the olivine treatment consistently had lower concentrations of inorganic carbon in the first 30 cm of the profile (lower by 0.6 ($p = 0.999$; see comment in Table S4) and 0.4% ($p = 0.990$) respectively; Fig. 5A), suggesting carbonate dissolution over the course of the experiment. Total organic carbon content of the soil in all three columns decreased from a maximum concentration (~6.5% in the initial material) near the surface to a minimum deeper in the column (<0.1%, D.L. in control column), although there was no consistent change over the course of the experiment (Fig. 5B). These values are typical for calcareous soils (Chichester and Chaison, 1992).

4.4. Geochemical modelling

PHREEQC v2 (Parkhurst and Appelo, 1999 using llnl.dat database) was used to investigate the saturation states of various solid phases in the effluent solution samples. All solutions were undersaturated with respect to Mg silicate (and hydrated) phases (e.g. forsterite, talc), and oversaturated with respect to clay (e.g. kaolinite, montmorillonite) and alumina (e.g. gibbsite, diaspore) minerals. By assuming charge balance between the anions in the input

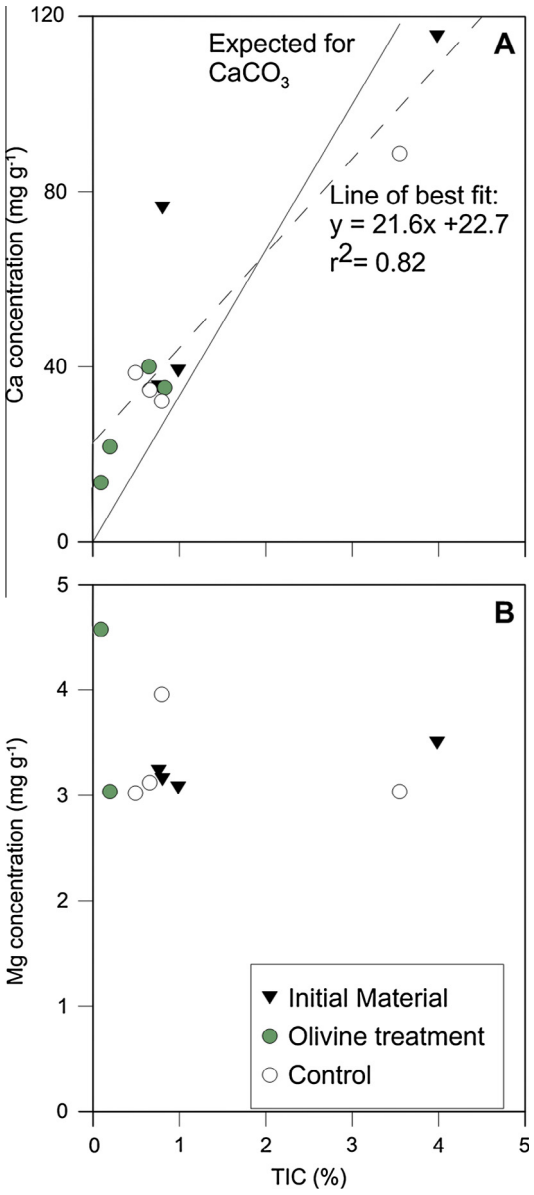

Fig. 4. Total (A) Ca and (B) Mg concentration of the soil plotted against total inorganic carbon. The solid black line represents the relationship that might be expected for $CaCO_3$. The dashed line is a line of best fit through the data.

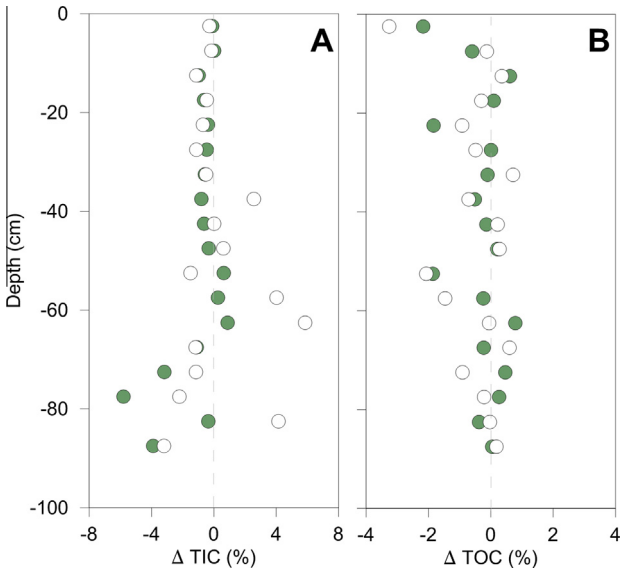

Fig. 5. Changes from the initial material in (A) inorganic and (B) organic carbon concentration through the soil profile (error bars are within the size of the symbols).

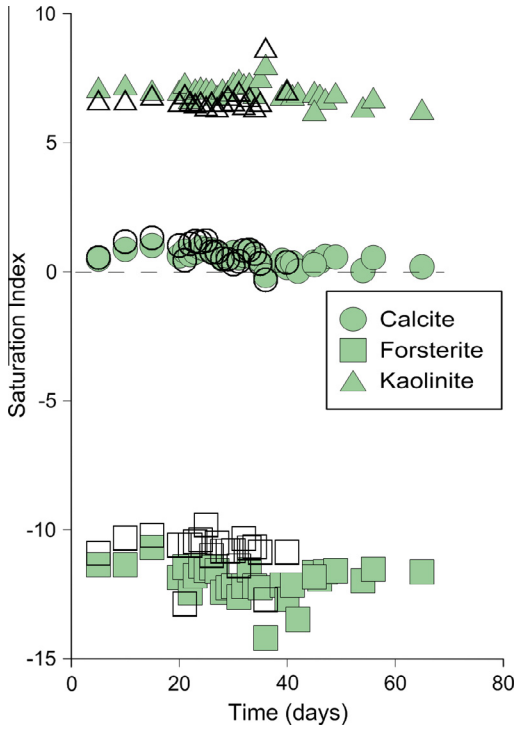

Fig. 6. Results from PHREEQC modelling showing the saturation indices of kaolinite, calcite, and forsterite over time. Solid and open shapes represent the olivine and control treatments respectively.

solution (SO_4^{2-}, PO_4^{3-}, NO_3^-) and the effluent cation concentration, it was possible to estimate the saturation states of carbonate minerals. The model predicts some oversaturation with respect to calcite and dolomite. However, other Mg carbonate minerals (e.g. hydromagnesite, nesquehonite) are undersaturated. A summary of this information is provided in Fig. 6.

5. Discussion

5.1. Dissolution rate

Three types of mineral phases may be dissolving in the soil columns: existing soil carbonate, existing soil silicates, and the added silicate–olivine in the treated column. Comparison of Mg, Ca, and Si concentrations in the effluent waters enables assessment of the net dissolution rates of these three phases. Note that these are net values: any formation of secondary minerals, or surface adsorption of cations on existing minerals, will reduce effluent cation concentrations. Initial dissolution rates of mineral phases might therefore be higher than calculated here, but the calculations are highly relevant to the field setting in which secondary mineralisation and surface sorption will also occur.

Solutions from both the control and olivine-treated columns show a strong relationship between Ca and Mg concentration (Fig. 7A). The relationship for the untreated column is well explained by progressive dissolution of existing carbonate in the soil, having a slope indicative of the mass ratio in that carbonate phase as assessed from the bulk measurements (Fig. 7A). Such dissolution is also evident from the decrease in TIC observed in both

columns. In the olivine-treated column, solution Mg concentrations are higher than those from the control by ≈2.6 μg g^{-1}, indicating that an additional Mg-rich phase is also dissolving – very likely the added olivine.

Mg covaries with Si in effluent from the olivine-treated column (Fig. 7B), with a gradient similar to the mass ratio of Si:Mg in the added olivine (~1.5). After 80 days, the $\Delta Mg/Ca_{olivine\ treated-control}$ starts to rapidly increase, suggesting that drip-waters from the olivine-treated column have rapidly increasing Mg concentrations, relative to Ca derived from carbonate. The likelihood of olivine dissolving in the treated experiment is also indicated by PHREEQC calculations using the measured solution chemistries, which showed that forsterite was undersaturated in all solutions. Secondary minerals such as kaolinite were oversaturated, indicating that they are likely to precipitate. However, the sodium acetate leach of the post-treated material suggests that a negligible amount of Mg was incorporated interstitially.

Assuming the difference between the Mg concentration in the effluent of the control and olivine-treated columns is wholly derived from dissolution of the added olivine, surface area normalised dissolution rates, and their change with time, can be calculated for the olivine (Eq. (2); Fig. 7C). The dissolution rate increased from $10^{-16.4}$ to $10^{-15.5}$ moles(Mg) cm^{-2} s^{-1} within the first 50 days and remained relatively constant thereafter (between $10^{-15.9}$ and $10^{-15.6}$ moles(Mg) cm^{-2} s^{-1}. This range remains consistent when the 2:1 molar ratio Mg:olivine is accounted for ($10^{-16.7}$–$10^{-15.8}$ moles(olivine) cm^{-2} s^{-1})

$$W_r = \frac{Q([Mg^{2+}]_{olivine} - [Mg^{2+}]_{control})}{SSA} \quad (2)$$

where W_r is the material surface area normalised dissolution rate (moles(Mg) cm^{-2} s^{-1}), Q is the solution flux through the column (g s^{-1}), [Mg^{2+}] is the molar concentration of Mg in the olivine and control (moles g^{-1}), and SSA is the specific surface area of the material (cm^2 g^{-1}, 3.04×10^4).

The rate of olivine dissolution in the column experiments of this study is 10–100 times slower than that predicted from laboratory derived kinetics for forsterite dissolution (10^{-14} at 19 °C and pH 7 (Palandri and Kharaka, 2004)). This demonstrates that laboratory experiments on single mineral phases, while valuable for constraining particular aspects of dissolution kinetics, fail to fully replicate the suite of processes occurring in the soil environment. The soil column approach followed in this study makes it more challenging to identify individual processes (e.g. secondary mineral formation) but allows an assessment of the net release of cations from mineral dissolution in a soil environment, while still being able to manipulate, control, and monitor the environment of that soil very closely. This approach is therefore well suited to establishing the expected impact of addition of minerals phases to the soil environment.

Net dissolution rates of olivine from these experiments can also be converted into an expected catchment scale weathering rate ($W_{r\text{-}cat}$, in t(olivine) km^{-2} a^{-1}) through Eq. (3).

$$W_{r\text{-}cat} = \frac{SSA \cdot M_{oliv} \cdot W_r \cdot 10^7}{MgO \cdot CSA_{col}} \cdot (12144 \cdot 10^4) \quad (3)$$

where, M_{oliv} is the mass of olivine added to the column (g, 100), MgO is the mass% of magnesium in the material (expressed as % MgO, 47.7), and CSA_{col} is the cross sectional area of the column (m^2, $10^{-2.11}$). A mineral surface area normalised dissolution rate of $10^{-15.7}$ moles(Mg) cm^{-2} s^{-1} equates to a spatial area normalised dissolution rate of 200 t(olivine) km^{-2} a^{-1}. This is an order of magnitude more rapid than the global average catchment scale derived rates (24 t km^{-2} a^{-1} Gaillardet et al., 1999), but similar to the most rapid chemical denudation rates from volcanic island arcs

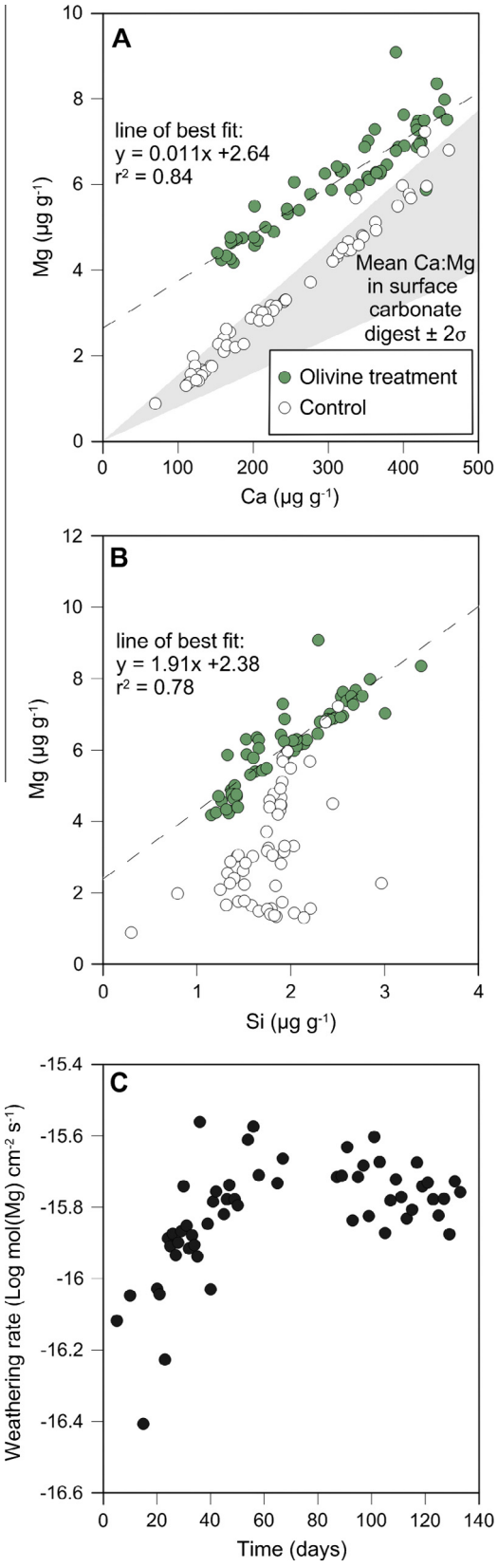

Fig. 7. Relationship between (A) Ca and Mg, and (B) Si and Mg in the effluent solutions of the olivine treated and control columns The bold lines in A represent 2σ about the mean of Ca:Mg determined from step 2 (carbonate) in the sequential extraction, indicating that, for the control experiment, dissolution of original carbonate well explains the observations. The dashed line is a best fit to the data from the olivine-treated column. (C) The surface area normalised dissolution rate of the olivine over the duration of the experiment.

(100s t km^{-2} a^{-1}; Gaillardet et al., 2011). This is perhaps not surprising, given that the freshly ground olivine material used in these experiments is similarly unstable at surface-Earth conditions as volcanic material.

5.2. Enhanced weathering as a greenhouse gas removal technology

One application of the dissolution rate of olivine measured in this study is to assess the possible suitability of widespread olivine addition to soils as an intentional enhanced weathering approach to draw CO_2 from the atmosphere. Such enhanced weathering would depend on environmental variables, such as temperature and rainfall, and also on the amount and particle size of olivine added to soil. The surface-area-normalised dissolution rates of this study can be used to assess the impact of changes in the grain size on the release of cations to the soil from added olivine.

In previous research, the feasibility assessment of enhanced weathering has focused on the calculation of energy and carbon balances (Renforth, 2012; Hangx and Spiers, 2009; Moosdorf et al., 2014; Köhler et al., 2010). While a number of factors contribute (e.g. extraction, transport, application), the largest uncertainty is the energy requirements of material comminution (Renforth, 2012). Comminution is required to decrease the material particle size and increase the weathering surface area. However, given the lack of clarity about the most suitable values to use for dissolution kinetics in the soil environment, it has been unclear how much surface area is required for a desired CO_2 uptake. For a given extent of dissolution (X), the initial particle diameter (D_0; m) can be related to dissolution rate (W_r; moles(mineral) m^{-2} s^{-1}) through a shrinking core model (Eq. (4)).

$$X(t) = \frac{D_0^3 - (D_0 - 2W_r V_m t)^3}{D_0^3} \tag{4}$$

where V_m is the molar volume of the material (m^3 $mole^{-1}$), and t is the dissolution time (s). Grinding activity does not produce a single particle size, therefore, the above equation should be integrated over a particle size distribution. Here we use a normalised gamma distribution (Eq. (5)) which has previously been coupled to a shrinking core model (Gbor and Jia, 2004)

$$\Gamma(D) = \frac{D^{\alpha-1} e^{-D/\beta}}{\beta^{\alpha}\Gamma(\alpha)} \tag{5}$$

where α and β are empirically derived coefficients that describe the variability of particle size (see Gbor and Jia, 2004). With the dissolution rates assessed from this study ($\sim 10^{-16}$ moles cm^{-2} s^{-1}) an initial P_{80} particle diameter (the diameter to which 80% of the product passes) on the order of 0.01–0.1 μm is required for complete dissolution in 5 years. Although this assumes a geometric surface area, which can be an order of magnitude smaller than those determined through gas absorption (e.g. calculated from Brantley and Mellott, 2000). Therefore, a P_{80} particle diameter of ~1 μm may be sufficient. Grinding is inherently inefficient at creating new surface area, requiring around 10^{-4} MJ of electrical energy per m^2 (compared to a thermodynamic minimum for forsterite of 10^{-6} MJ; Swain and Atkinson, 1978). Therefore, grinding to <1 μm will require >1.5 GJ t^{-1}. When combined with other production processes (using the values in Renforth, 2012; Moosdorf et al., 2014)), the energy requirements for enhanced weathering may be on the order of 6 GJ per net tonne of CO_2 sequestered (resolved as total thermal energy). This is of the same order as the ~1–10 GJ tCO_2^{-1} for removing CO_2 from the atmosphere through chemical scrubbing ('Direct Air Capture'; House et al., 2011; Keith et al., 2006; Lackner, 2009) or ocean liming (Renforth et al., 2013; Renforth and Kruger, 2013).

This study used elevated and constant solution flux (30× typical Oxfordshire rainfall), for a discrete soil type (calcareous soil), at a fixed temperature (19 °C). The solutions in the experiments were shown to be undersaturated with respect to forsterite, and over saturated with respect to clay minerals. At lower or intermittent flux, the solutions will likely be closer to equilibrium with the added mineral, and/or a passivating layer of secondary clay minerals may precipitate over the added mineral surface. Considering this, slower dissolution kinetics may be expected at more realistic solution fluxes. For a comprehensive assessment of terrestrial enhanced weathering, the experiment described here should be replicated for a broader range of variables.

The results of this study also have implications for the use of K-bearing silicates as replacement fertilisers. At an equivalent pH and temperature, Palandri and Kharaka (2004) predict K-feldspar and biotite will dissolve two orders of magnitude slower than forsterite. As such, initial particle diameters ≪0.5 μm may be required to facilitate almost complete dissolution in the same time period, with an energy requirement on the order of 2.5 GJ t^{-1}. Being able to effectively audit carbon sequestration in an up-scaled enhanced weathering technology is a considerable challenge (see Hartmann et al., 2013). A chemical monitoring system would need to be created in catchments where enhanced weathering was deployed. Furthermore, a method for distinguishing between the weathering of the added mineral and the background weathering would need to be established.

5.3. Environmental impact from trace metals

A number of workers have suggested that the release of potentially toxic elements during the dissolution of olivine may pose an environmental risk which would subsequently lower the potential of terrestrial enhanced weathering (Hartmann et al., 2013; Renforth, 2012). From the results of this study, there was elevated Cr in 5 of the solution samples from the olivine column, the remaining samples showed no difference compared to the control. Ni was measured but was below the detection limit in all of the effluent solutions. The Mg/Ni and Mg/Cr of the olivine was approximately 106 and 263 respectively. Assuming stoichiometric dissolution, the Mg concentrations derived from olivine weathering (1–5 μg g^{-1}) would yield concentrations between 7 and 46 ng g^{-1} for Ni and 3 an 19 ng g^{-1} for Cr, (which is well above the 0.3 and 0.1 ng g^{-1} LoQ). This suggests that >99% of these trace elements are retained within the soil, which is unsurprising given the high concentration of these elements in very mature soils such as laterites (e.g. Lewis et al., 2006), implying that the short term environmental impact of trace metals from the added olivine may be limited. However, the long-term accumulation of these elements may pose an environmental risk, which could eventually limit the application. For instance, assuming a maximum threshold value of ~100 mgNi kg(soil)$^{-1}$ (e.g. Environment Agency, 2009 and assuming a soil density of 1.5 t m^{-3}, and an accumulation depth of 20 cm), the maximum application potential for olivine (containing ~3 gNi kg^{-1}; De Hoog et al., 2010), is 95 t ha^{-1} (although this rises to ~500 tonnes if accumulation depth extends down to 1 m in the soil profile. The same calculation for Cr using a 100 mgCr kg(soil)$^{-1}$ threshold value, and 150 mgCr kg^{-1} of olivine, allows for an maximum application of 2000 t ha^{-1}. The appropriateness of these threshold values requires further evaluation to understand the bioavailability of the heavy metals contained in the olivine and the accumulation depth in the soil profile.

6. Conclusion

By bringing a soil profile into the laboratory, we have assessed the rate of olivine dissolution without diminishing the complexity

of the soil environment, and attempted to bridge the gap between laboratory assessment of mineral dissolution rates and catchment scale assessment of chemical weathering rates. Assessment of changes in the solid phase of soils is unlikely to be realistic on laboratory timescales, but mineral dissolution rates can be constrained by chemical analysis of the solution exiting the base of the soil. We derive a surface area normalised dissolution rate of $10^{-16.4}$ to $10^{-15.5}$ moles(Mg) cm^{-2} s^{-1} for a forsterite rich olivine, equivalent to $\sim$200 t km^{-2} a^{-1} when normalised to land area. This is more than an order of magnitude slower than the rate of olivine dissolution predicted from laboratory derived kinetics, and at the high end of weathering rates in natural volcanic terrains. One application of this dissolution rate is to assess the potential for enhanced weathering as a carbon mitigation strategy. Simple calculations indicate that it would be necessary to grind olivine to a particle size of 1 μm or less to enable dissolution in 1–5 years, requiring grinding energy of around 1.5 GJ (electrical) per tonne of rock (comparable with the more extensively studied alternatives for CO_2 uptake such as direct air capture). The experimental design used in this study has potential for much wider assessment of weathering rates in natural and manipulated soils, and provides an assessment of olivine weathering of use for modelling of catchment and global geochemical fluxes.

Acknowledgements

PR and GMH acknowledge generous funding from the Oxford Martin School through the Oxford Geoengineering Programme, and from the Hay Family. PPvS acknowledges funding from NERC Research Fellowship NE/I020571/1. The authors would like to thank Rob Ainsworth and Graeme Jackson (SoilsLimited) and James Price (Perdiswell Farm) for their help with core extraction. Thomas Phelan and Nicolas Boheim (University of Oxford) are thanked for their help with experimental construction and sample collection. Neil Rowson (University of Birmingham) is thanked for his help with olivine comminution. Phil Holdship, Steve Wyatt (University of Oxford) and Nick Marsh (University of Leicester) are thanked for their assistance during analysis.

Appendix A. Supplementary material

Supplementary data associated with this article can be found, in the online version, at http://dx.doi.org/10.1016/j.apgeochem.2015.05.016.

References

Berner, R.A., Kothavala, Z., 2001. Geocarb III: a revised model of atmospheric CO_2 over phanerozoic time. Am. J. Sci. 301, 182–204.
Brantley, S.L., Mellott, N.P., 2000. Surface area and porosity of primary silicate minerals. Am. Mineral. 85, 1767–1783.
Calmels, D., Galy, A., Hovius, N., Bickle, M., West, A.J., Chen, M.-C., Chapman, H., 2011. Contribution of deep groundwater to the weathering budget in a rapidly eroding mountain belt, Taiwan. Earth Planet. Sci. Lett. 303, 48–58.
Chichester, F.W., Chaison, R.F.J., 1992. Analysis of carbon in calcareous soils using a two temperature dry combustion infrared instrumental procedure. Soil Sci. 153, 237–241.
De Hoog, J.C.M., Gall, L., Cornell, D.H., 2010. Trace-element geochemistry of mantle olivine and application to mantle petrogenesis and geothermobarometry. Chem. Geol. 270, 196–215.
Environment Agency, 2009. Soil Guideline Values for Nickel in Soil. Environment Agency. Science Report SC050021.
Gaillardet, J., Dupré, B., Louvat, P., Allègre, C.J., 1999. Global silicate weathering and CO_2 consumption rates deduced from the chemistry of large rivers. Chem. Geol. 159, 3–30.
Gaillardet, J., Louvat, P., Lajeunesse, E., 2011. Rivers from Volcanic Island Arcs: the subduction weathering factory. Appl. Geochem. 26 (Supplement), S350–S353.
Gbor, P.K., Jia, C.Q., 2004. Critical evaluation of coupling particle size distribution with the shrinking core model. Chem. Eng. Sci. 59, 1979–1987.
Hangx, S.J.T., Spiers, C.J., 2009. Coastal spreading of olivine to control atmospheric CO_2 concentrations: a critical analysis of viability. Int. J. Greenhouse Gas Con. 3, 757–767.
Hartmann, J., West, A.J., Renforth, P., Köhler, P., De La Rocha, C.L., Wolf-Gladrow, D.A., Dürr, H.H., Scheffran, J., 2013. Enhanced chemical weathering as a geoengineering strategy to reduce atmospheric carbon dioxide, supply nutrients, and mitigate ocean acidification. Rev. Geophys. 51, 113–149.
Harvey, L.D.D., 2008. Mitigating the atmospheric CO_2 increase and ocean acidification by adding limestone powder to upwelling regions. J. Geophys. Res. 113, C04028.
Holdren, G.R., Speyer, P.M., 1985. Reaction rate-surface area relationships during the early stages of weathering—I. Initial observations. Geochim. Cosmochim. Acta 49, 675–681.
House, K.Z., Baclig, A.C., Ranjan, M., van Nierop, E.A., Wilcox, J., Herzog, H.J., 2011. Economic and energetic analysis of capturing CO_2 from ambient air. Proc. Natl. Acad. Sci. 108, 20428–20433.
Keith, D.W., Ha-Duong, M., Stolaroff, J.K., 2006. Climate strategy with CO_2 capture from the air. Clim. Change 74, 17–45.
Kheshgi, H.S., 1995. Sequestering atmospheric carbon dioxide by increasing ocean alkalinity. Energy 20, 915–922.
Köhler, P., Hartmann, J., Wolf-Gladrow, D.A., 2010. Geoengineering potential of artificially enhanced silicate weathering of olivine. Proc. Natl. Acad. Sci. 107, 20228–20233.
Köhler, P., Abrams, J.F., Völker, C., Hauck, J., Wolf-Gladrow, D.A., 2013. Geoengineering impact of open ocean dissolution of olivine on atmospheric CO_2, surface ocean pH and marine biology. Environ. Res. Lett. 8, 014009.
Lackner, K.S., 2009. Capture of carbon dioxide from ambient air. Eur. Phys. J-Spec. Top. 176, 93–106.
Lewis, J.F., Draper, G., Proenza, J.A., Espaillat, J., Jimenez, J., 2006. Ophiolite-related ultramafic rocks (serpentinites) in the Caribbean Region: a review of their occurrence, composition, origin, emplacement and Ni-laterite soil formation. Geol. Acta 4, 237–263.
Lundström, U., 1990. Laboratory and lysimeter studies of chemical weathering. The Surface Waters Acidification Programme, pp. 267–274.
Manning, D.A.C., 2008. Biological enhancement of soil carbonate precipitation: passive removal of atmospheric CO_2. Mineral. Mag. 72, 639–649.
Manning, D.A.C., Renforth, P., 2012. Passive sequestration of atmospheric CO_2 through coupled plant-mineral reactions in urban soils. Environ. Sci. Technol. 47, 135–141.
Manning, D.A.C., Renforth, P., Lopez-Capel, E., Robertson, S., Ghazireh, N., 2013. Carbonate precipitation in artificial soils produced from 'wastes': an opportunity for passive carbon sequestration. Int. J. Greenhouse Gas Control 17, 309–317.
Moosdorf, N., Renforth, P., Hartmann, J., 2014. Carbon dioxide efficiency of terrestrial enhanced weathering. Environ. Sci. Technol. 48, 4809–4816.
Nagy, K.L., Blum, A.E., Lasaga, A.C., 1991. Dissolution and precipitation kinetics of kaolinite at 80 degrees C and pH 3; the dependence on solution saturation state. Am. J. Sci. 291, 649–686.
Pačes, T., 1983. Rate constants of dissolution derived from the measurements of mass balance in hydrological catchments. Geochim. Cosmochim. Acta 47, 1855–1863.
Palandri, J.L., Kharaka, Y.K., 2004. A complitation of rate parameters of water-mineral interaction kinetics for application to geochemical modelling. United States Geological Survey.
Parkhurst D.L. and Appelo C.A.J. (1999) User's guide to PHREEQC (Version 2): a computer program for speciation, batch-reaction, one-dimensional transport, and inverse geochemical calculations. Water-Resources Investigations Report. US Geological Survey.
Peters, S.C., Blum, J.D., Driscoll, C.T., Likens, G.E., 2004. Dissolution of wollastonite during the experimental manipulation of Hubbard Brook Watershed 1. Biogeochemistry 67, 309–329.
Pokrovsky, O.S., Schott, J., 2000. Kinetics and mechanism of forsterite dissolution at 25 °C and pH from 1 to 12. Geochim. Cosmochim. Acta 64, 3313–3325.
Rau, G.H., 2011. CO_2 mitigation via capture and chemical conversion in seawater. Environ. Sci. Technol. 45, 1088–1092.
Renforth, P., 2012. The potential of enhanced weathering in the UK. Int. J. Greenhouse Gas Control 10, 229–243.
Renforth, P., Kruger, T., 2013. Coupling mineral carbonation and ocean liming. Energy Fuel. 27, 4199–4207.
Renforth, P., Jenkins, B.G., Kruger, T., 2013. Engineering challenges of ocean liming. Energy 60, 442–452.
Schuiling, R.D., de Boer, P.L., 2010. Coastal spreading of olivine to control atmospheric CO_2 concentrations: a critical analysis of viability. Comment: nature and laboratory models are different. Int. J. Greenhouse Gas Control 4, 855–856.
Schuiling, R.D., Krijgsman, P., 2006. Enhanced weathering: an effective and cheap tool to sequester CO_2. Clim. Change 74, 349–354.
Sigfusson, B., Paton, G.I., Gislason, S.R., 2006. The impact of sampling techniques on soil pore water carbon measurements of an Icelandic Histic Andosol. Sci. Total Environ. 369, 203–219.
Swain, M.V., Atkinson, B.K., 1978. Fracture surface energy of olivine. In: Byerlee, J., Wyss, M. (Eds.), Rock Friction and Earthquake Prediction. Birkhäuser, Basel.
ten Berge, H.F.M., van der Meer, H.G., Steenhuizen, J.W., Goedhart, P.W., Knops, P., Verhagen, J., 2012. Olivine ∗weathering in soil, and its effects on growth and nutrient uptake in ryegrass (*Lolium perenne* L.): a pot experiment. PLoS One 7, e42098.

Tessier, A., Campbell, P.G.C., Bisson, M., 1979. Sequential extraction procedure for the speciation of particulate trace metals. Anal. Chem. 51, 844–851.
van Hees, P.A.W., Lundström, U.S., Giesler, R., 2000. Low molecular weight organic acids and their Al-complexes in soil solution—composition, distribution and seasonal variation in three podzolized soils. Geoderma 94, 173–200.
Walker, J.C.G., Hays, P.B., Kasting, J.F., 1981. A negative feedback mechanism for the long-term stabilization of Earth's surface temperature. J. Geophys. Res-Oceans 86, 9776–9782.
White, A.F., Brantley, S.L., 1995. Chemical Weathering Rates of Silicate Minerals. Mineralogical Society of America. ISBN 0-939950-38-3.
White, A.F., Brantley, S.L., 2003. The effect of time on the weathering of silicate minerals: why do weathering rates differ in the laboratory and field? Chem. Geol. 202, 479–506.
White, A.F., Blum, A.E., Bullen, T.D., Vivit, D.V., Schulz, M., Fitzpatrick, J., 1999. The effect of temperature on experimental and natural chemical weathering rates of granitoid rocks. Geochim. Cosmochim. Acta 63, 3277–3291.